Geomicrobiological Redox Cycling of the Transuranic Element Neptunium

GARETH T. W. LAW,[†] ANDREA GEISSLER,[†,⊥] JONATHAN R. LLOYD,[†] FRANCIS R. LIVENS,[†,‡] CHRISTOPHER BOOTHMAN,[†] JAMES D. C. BEGG,[§,#] MELISSA A. DENECKE,[∥] JORG ROTHE,[∥] KATHY DARDENNE,[∥] IAN T. BURKE,[§] JOHN M. CHARNOCK,[†] AND KATHERINE MORRIS*[,†]

Research Centre for Radwaste and Decommissioning and Williamson Research Centre for Molecular Environmental Science, School of Earth, Atmospheric and Environmental Sciences, and Centre for Radiochemistry Research, School of Chemistry, The University of Manchester, Manchester, M13 9PL, U.K., Earth System Science Institute, School of Earth and Environment, University of Leeds, Leeds, LS2 9JT, U.K., and Karlsruhe Institute of Technology, Institut für Nukleare Entsorgung, D-76021-Karlsruhe, Germany

Received June 4, 2010. Revised manuscript received October 11, 2010. Accepted October 19, 2010.

Microbial processes can affect the environmental behavior of redox sensitive radionuclides, and understanding these reactions is essential for the safe management of radioactive wastes. Neptunium, an alpha-emitting transuranic element, is of particular importance because of its long half-life, high radiotoxicity, and relatively high solubility as $Np(V)O_2^+$ under oxic conditions. Here, we describe experiments to explore the biogeochemistry of Np where Np(V) was added to oxic sediment microcosms with indigenous microorganisms and anaerobically incubated. Enhanced Np removal to sediments occurred during microbially mediated metal reduction, and X-ray absorption spectroscopy showed this was due to reduction to poorly soluble Np(IV) on solids. In subsequent reoxidation experiments, sediment-associated Np(IV) was somewhat resistant to oxidative remobilization. These results demonstrate the influence of microbial processes on Np solubility and highlight the critical importance of radionuclide biogeochemistry in nuclear legacy management.

Introduction

Globally, the management of radioactive wastes from nuclear power generation and weapons production is a subject of intense public concern, and the prospect of a new generation of nuclear power plants only increases its significance. Neptunium (Np) is a transuranic element, and the dominant isotope, ^{237}Np, has a long half-life (2.13×10^6 years) and high biological toxicity. In geological disposal, Np is one of the most radiologically significant contaminants (*1*−*3*). The environmental chemistry of Np is dominated by its redox chemistry. Under oxic conditions, the dioxygenyl, neptunyl species ($Np(V)O_2^+$) dominates and is poorly sorbed to mineral surfaces, making Np(V) very mobile (*1, 2, 4, 5*). In contrast, under-reducing conditions, Np(IV) species are expected to dominate and Np(IV) can be removed from solution by hydrolysis and reaction with surfaces (*1, 2*).

In both natural and engineered environments, microbially mediated processes control the redox chemistry of the shallow subsurface (*6*). These processes are also likely to be significant in the deep geological settings that will host geological disposal facilities (*7*). Thus biogeochemical reactions may critically enhance or reduce the solubility of Np and other redox active radionuclides. Indeed, recent work has shown that a range of sediment bacteria can mediate radionuclide redox transformations (e.g., refs *4* and *8*). However, to now, studies have focused on uranium and technetium because of their experimental accessibility and significance in contaminated land (*4*). This work has shown that biotransformations of radionuclides are complex and can proceed via enzymatic interactions at the metal/microbe interface or via abiotic reaction with microbial reduction products (e.g., Fe(II) or sulfur species) (*4, 8*). Currently, there are only a handful of studies on transuranic geomicrobiology (*9*−*15*) and to our knowledge no biogeochemical studies exist with heterogeneous environmental samples, complete with indigenous microbial communities. Regardless, initial work has highlighted the subtleties of Np behavior, with axenic culture experiments showing varying species specific capability for Np(V) bioreduction and biotoxicity at low millimolar concentrations (*9, 11, 13*). Against this complex background we have examined the biocycling behavior of Np in nuclear site sediments with indigenous microbial communities to further constrain the uncertainties associated with Np biogeochemistry.

Experimental Section

Safety. ^{237}Np is a radioactive alpha emitter with beta/gamma-emitting daughter isotopes. Radioisotopes should be handled by suitably qualified and experienced personnel in a properly equipped laboratory, and any work should follow appropriate risk assessment. The possession and use of radioactive materials is subject to statutory controls.

Sediment Collection, Storage, and Characterization. Sediment was collected from an area located approximately 2 km from the Sellafield site (*16*). The collected material was representative of the Quaternary unconsolidated alluvial flood plain deposits that underlie Sellafield. The sediments (herein 'Sellafield sediment') were transferred directly into a sterile HDPE container, sealed, and stored at 5 °C in darkness. Experiments began within one month of sampling.

Np(V) Preparation. A molar excess of sodium hydroxide was added to a mixed oxidation, radiochemically pure ^{237}Np solution (LEA-CERCA, France). The resulting Np precipitate was washed three times in deionized water, dissolved in 6 M HNO_3, and gently heated to facilitate oxidation to Np(V). After visible color change (olive green to emerald green, indicative of Np(V)) the Np was reprecipitated with NaOH, washed three times with deionized water, and finally dissolved in 0.1 M HCl. A UV−vis-NIR (Varian, Cary 500) spectrum confirmed speciation as Np(V) with diagnostic Np(V) peaks present at 618 and 980 nm and no contribution from Np(IV) absorption peaks at 723 and 960 nm (*17*).

* Corresponding author phone: +44 161 275 7541; fax: +44 161 306 9361; e-mail: katherine.morris@manchester.ac.uk.
[†] School of Earth, Atmospheric and Environmental Sciences, The University of Manchester.
[‡] School of Chemistry, The University of Manchester.
[§] University of Leeds.
[∥] Institut für Nukleare Entsorgung.
[⊥] Present address: Institute of Radiochemistry, Forschungszentrum Rossendorf, D01314-Dresden, Germany.
[#] Present address: Glenn T. Seaborg Institute, Lawrence Livermore National Laboratory, Livermore, CA 94550.

10.1021/es101911v

Published on Web 11/03/2010

Low-Level Neptunium Bioreduction Microcosms. Bioreduction microcosms were prepared using a synthetic groundwater representative of the Sellafield region (*16, 18*) (see Supporting Information for composition) and Sellafield sediment. Previous experiments (*16*) highlighted that the indigenous sediment electron donor(s) could not support bioreduction over the time scales of the experiments; consequently, 10 mM sodium acetate was added to the groundwater as an electron donor. After formulation, the groundwater was sterilized by autoclaving (1 h at 120 °C), sparged with filtered 80/20 N_2/CO_2, and pH adjusted to ~7.0 via addition of 0.01 M HCl to provide optimum conditions for geomicrobiological processes (*16*). All experiments were run in triplicate. Np(V) was injected into oxic, sterile synthetic groundwater; oxic, heat-killed (autoclaved for 20 min, three times, at 120 °C) control microcosms; and oxic, microbially active sediment microcosms, to a final concentration of 2 μM (sediment: solution ratio 1: 10). To induce bioreduction, the microcosm headspace was sparged with 80/20 N_2/CO_2, crimp-sealed, and then incubated anaerobically at 21 °C. During incubation, the microcosms were periodically sampled using aseptic technique with sterile Ar-flushed syringes, and porewater and sediment samples were collected from the slurry via centrifugation under Ar (15 000*g*, 10 min). Porewaters were then sampled for total Np, NO_3^-, NO_2^-, Fe, Mn, pH, and Eh. Sediment samples were analyzed for 0.5 N HCl-extractable Fe(II) and total Fe to estimate microbially produced Fe(II) ingrowth into sediments. A 0.2 g aliquot of untreated sediment was also sampled and stored under sterile conditions at −80 °C for microbiological characterization.

X-ray Absorption Spectroscopy Bioreduction and Reoxidation Microcosms. Experiments for XAS analysis required higher Np concentrations to allow detection (several hundred ppm on solids). Two separate bioreduction treatments were prepared: (i) a progressive bioreduction system, and (ii) a poised bioreduction system. In both cases, microcosms were prepared as previously described (see above), but the microcosms consisted of 0.8 g of sediment and 8 mL of groundwater and were spiked with 0.2 mM Np(V). Additionally, 2 mM of NO_3^- was added to the groundwater to facilitate a longer period of denitrification. For the progressive treatment, Np(V) was spiked into a microbially active oxic microcosm, which was then incubated anaerobically at 21 °C until Fe(III)-reducing conditions were detected (40 days). Thereafter, the microcosm was frozen at −80 °C under Ar until XAS analysis. For the poised treatments, several ($n = 4$) microcosms were incubated anaerobically at 21 °C without Np and periodically sampled to monitor terminal electron-accepting processes. When denitrification or early metal-, Fe(III)-, or sulfate-reducing conditions were detected in successive microcosms, Np(V) was spiked into the microcosm which was then incubated for a further 10 days at 10 °C (temperature reduction slowed microbial metabolism, thus ensuring sampling under constrained TEAPs), geochemically sampled, and frozen under Ar at −80 °C until XAS analysis. Sterile control microcosms were also created. Here, both oxic and Fe(III)-reducing microcosms were autoclaved prior to Np(V) addition, incubated for 10 days at 10 °C, geochemically sampled, and then frozen under Ar at −80 °C until XAS analysis.

Reoxidation XAS experiments were also conducted. Here, Np-labeled progressive bioreduction samples (as described above) were incubated until ~95% of 0.5 N HCl-extractable Fe was present as Fe(II). Thereafter, the microcosms either underwent daily injections of air into the headspace to provide air (O_2) oxidation samples or were injected with 25 mM NO_3^- to provide nitrate oxidation samples (*19*). An additional sterile control microcosm was also created; here, a Fe(III)-reducing microcosm was sterilized by autoclaving (3 × 120 °C for 20 min), spiked with Np(V), incubated for 10 days, and then injected with 25 mM $NaNO_3$.

Geochemical Analyses. Neptunium concentrations were determined by ICP-MS (VG PlasmaQuad 2) for low-level bioreduction samples and by liquid scintillation counting (Packard Tricarb 2100TR) for XAS samples. Porewater Np speciation was measured in select (early metal, Fe (III) reducing, and oxidation) XAS samples via TTA extraction (*20*). Total dissolved Fe, Mn, and NO_2^- concentrations were measured with standard UV−vis spectroscopy methods on a Cecil CE 3021 spectrophotometer (*21*−*23*). In low-level samples, aqueous NO_3^- and SO_4^{2-} were measured by ion chromatography (*24*). Aqueous NO_3^- and SO_4^{2-} could not be measured in XAS experiments because of radiological safety considerations; instead, porewater NO_2^- was used to monitor the occurrence of denitrification, and sediment blackening was presumed to be indicative of SO_4^{2-} reduction. Total bioavailable Fe(III) and the proportion of extractable Fe(II) in the sediment was estimated by digestion of 0.1 g of sediment in 5 mL of 0.5 N HCl for 60 min, with and without hydroxylamine, respectively, followed by colorimetric assay (*25*). Eh and pH were measured with an Orion 420A digital meter and calibrated electrodes. Standards were routinely used to check the reliability of all methods and calibration regressions had $R^2 \geq 0.99$.

DNA Extraction, Ribosomal Intergenic Spacer, and 16S rRNA Gene Analysis. Microbial community DNA was extracted from sediment samples (0.2 g) using the PowerSoil DNA Isolation Kit (Cambio, UK). The 16S−23S intergenic spacer region from the bacterial RNA operon was amplified from community DNA by PCR using primers S-D-Bact-1522-b-S-20 (eubacterial 16S rRNA small subunit) and L-D-Bact-132-a-A-18 (eubacterial 23S rRNA large subunit) (*26*). Amplification was performed in a BioRad iCycler (BioRad, UK) (*26*) with 35 cycles. The amplified products were separated by electrophoresis in a 3% tris-acetate-EDTA (TAE) gel. DNA was stained with ethidium bromide and viewed under shortwave UV light using a BioRad Geldoc 2000 system (BioRad, UK). Universal bacterial primers 8F (*27*) (5′AGAGTTTGATCCTGGCTCAG-3′) and 1492R (*28*) (5′TACGGYTACCTTGTTACGACTT-3′) were used to amplify 16S rRNA gene fragments from the extracted and purified chromosomal DNA. PCR was performed with an BioRad iCycler using 0.25 μM of each primer, 0.2 mM dNTPs, 1 × PCR buffer, 2.5 mM $MgCl_2$, and 1.25 units of JumpStart *Taq* DNA Polymerase (Sigma, UK), which was made up to a final volume of 50 μL with sterile water. The PCR amplification protocol was as follows: initial denaturation (94 °C, 4 min), 35 cycles of denaturation (94 °C, 30 s), annealing (57 °C, 30 s), elongation (72 °C, 1 min), and final extension (72 °C, 10 min). Amplified gene fragments were used for cloning in *E. coli* by using the StrataClone PCR Cloning Kit (Stratagene, UK). A total of ~96 white colonies per sample were randomly selected and sequenced. The gene products of the clones were purified with Shrimp Alkaline Phosphatase (SAP) (Promega, UK) and Exonuclease I (New England Biolabs, UK), and directly sequenced using an ABI Prism Big Dye Terminator Cycle Sequencing Kit (Applied Biosystems, UK), following the manufacturer's instructions. Sequences were obtained using the primer 1492r. DNA sequences were determined on an automated sequencer (ABI Prism 877 Integrated Thermal Cycler and ABI Prism 377 DNA Sequencer, Applied Biosystems, UK) and compared with those available in the GenBank by using BLAST (*29*) analysis (Basic Local Alignment Search Tool). Potential chimera formation was checked and excluded from final analysis using the Check_Chimera program of the RDP (*30*) (Ribosomal Database Project). Phylogenetic affiliation of the 16S rRNA gene sequences was estimated by BLAST and the Classifier function in RDP.

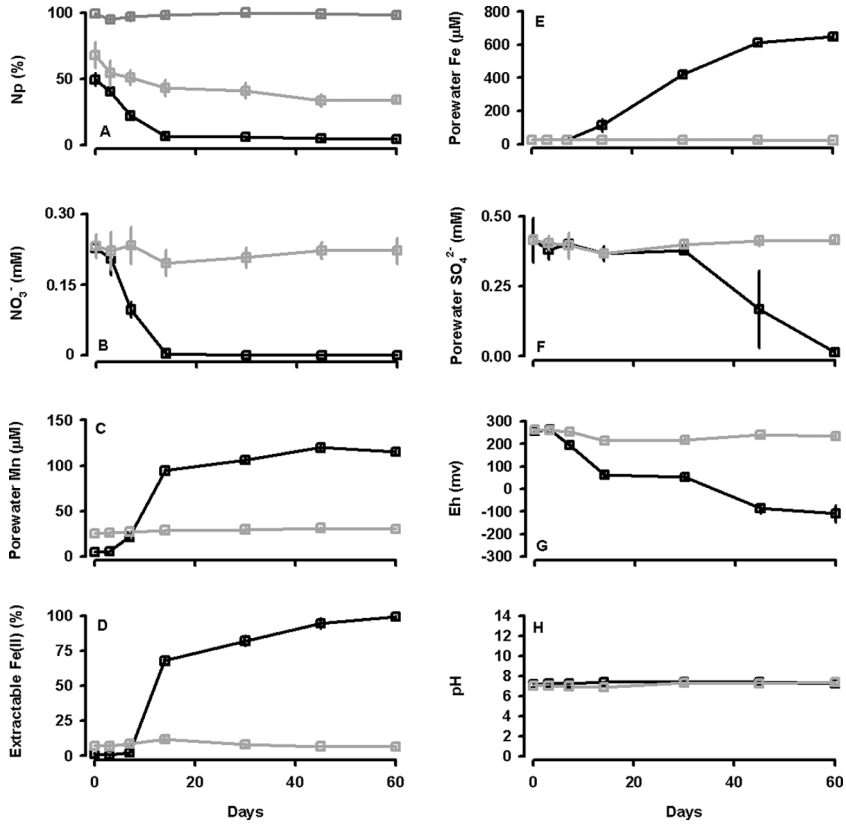

FIGURE 1. Bioreduction of Sellafield sediments showing enhanced removal of Np during early metal reduction. (A) % Np in solution, (B) NO_3^-, (C) porewater Mn, (D) % 0.5 N HCl-extractable sediment Fe as Fe(II), (E) porewater Fe, (F) SO_4^{2-}, (G) Eh, and (H) pH. Dark gray squares/trace = groundwaters (no sediment); light gray squares/trace = sterile control experiments; black squares/trace = microbially active experiments. Error bars are 1 σ of triplicate results (where not shown, errors are within the symbol size).

XAS Analysis. Sediment slurry was defrosted and centrifuged (12 min, 2000 g). Approximately 0.5 g of sediment (water content <50%) was then mounted for XAS analysis in an airtight XAS sample cell. The sample cell was then triple contained in heat-sealed vacuum bags and stored frozen under Ar until analysis. Where appropriate, sample manipulations were conducted under an O_2 free atmosphere. XAS analysis was conduced at the INE Beamline for actinide research at the ANKA synchrotron light source, Germany (*31*). Neptunium L_{III} edge spectra (17.610 keV) were collected in fluorescence mode by a 5 pixel solid-state detector (LEGe Canberra) using Ge(422) monochromator crystals. Energy calibration was completed by parallel measurement of a Zr foil. A total of 7−10 spectra were collected per sample. XANES spectra were collected for all samples, and EXAFS data were collected for a subset of samples. Spectra were merged using ATHENA (*32*). The ionization energy, E_0, for background subtraction, as well as for conversion to *k*-space, was set to 17.610 keV, the position of the Np L_{III} white-line maximum. XANES spectra were obtained following background subtraction and normalization of the edge jump to unity. The EXAFS spectra were obtained following background subtraction using EXSPLINE. XANES spectra were modeled to provide an estimate of the average Np oxidation state using the linear combination fitting function of ATHENA (*32*). End-member spectra used in linear combination modeling were (1) oxic (Np(V)-like) sediments, and (2) sulfate-reduced (Np(IV)-like) sediments. The chosen end-member XANES spectra resembled non-matrix matched Np(V) and Np(IV) standards (Figure 2) and were used to minimize matrix artifacts.

EXAFS spectra were analyzed with EXCURV98 using full curved wave theory and multiple scattering (*33, 34*). Phase shifts were determined from ab initio calculations using Hedin−Lundqvist potentials and von Barth ground states (*35*). The data were fit in k^3 space by defining a theoretical model extracted from the relevant literature (*36*−*43*) and using whole integer values for backscattering shells. The *k*-range was limited to between 3 and 8 Å because of excessive noise in high *k*-space. Shells of backscattering atoms were added around a central Np atom and the least-squares residual (the *R* factor (*35*)) was minimized by refining the energy correction E_f (the fermi energy), the absorber/scatter distance, the Debye−Waller factor, and the number of atoms in each shell. Shells were only included in the model fit if the overall *R*-factor was improved by ≥5%. Further modeling information is provided in the Supporting Information.

Results and Discussion

Sediment Characteristics. Full sediment characteristics are given in ref *16*. Briefly, the sediment mineral content is dominated by quartz, sheet silicates (muscovite and chlorite), and feldspars (albite and microcline). The elemental composition is dominated by Si (34.0 wt %), with high concentrations of Al (5.8 wt %), Fe (3.1 wt %), and Mn (0.1 wt %) present. The particle composition is 53% sand, 42% silt, and 5% clay, the sediment pH is 5.5, and the TOC content is 0.56 ± 0.08 wt %.

Microbially Mediated Progressive Bioreduction and Neptunium Behavior. In the groundwater microcosms, Np was undersaturated and remained in solution over 60 days (Figure 1A, dark gray trace). In contrast, in the sterile sediment system, rapid and partial Np sorption to the sediment occurred, with ~30% of the Np spike removed to the sediment after 1 h (Figure 1A, light gray trace). By 30−45 days, Np uptake had increased to ~60%. Thereafter, the Np concentration in solution was constant up to 12 months. Similar, partial sorption of Np(V) to geomedia has been observed by other workers (e.g., ref *5*). Finally, no bioreduction was evident in the sterile controls (Figure 1B−H). In the microbially active

sediment microcosms, ~ 50% of the added Np sorbed to the sediment after 1 h under oxic conditions (Figure 1A, black trace). The following microbial processes then developed: denitrification, indicated by removal of NO_3^- from ~3−14 days (Figure 1B); manganese reduction, indicated by Mn(II) ingrowth into porewaters between ~3−14 days (Figure 1C); Fe(III) reduction, indicated by an increase in Fe(II) in sediment slurry from 7 days (Figure 1D) and porewaters from 7−14 days (Figure 1E); and finally sulfate reduction, indicated by removal of porewater SO_4^{2-} and the appearance of black areas in the sediment after ~30 days (Figure 1F). Sediment slurry Eh also decreased over time (Figure 1G) and pH remained constant (Figure 1H). The initially diverse indigenous microbial community (0 days; Supporting Information Table 3) also became dominated by *Beta-* and *Deltaproteobacteria* with time (14 and 60 days; Supporting Information Tables 4 and 5) which likely controlled the onset of metal reduction. Finally, during early metal reduction, there was enhanced removal of porewater Np compared to sterile controls (3−14 days; Figure 1A), with <5% of the original Np spike remaining in solution after 14 days.

Neptunium Fate during Bioreduction. Experiments were prepared to explore Np(V) behavior under different biogeochemical conditions using X-ray absorption spectroscopy. In the sterile oxic and denitrifying microcosms, Np uptake was limited (10−30%). For all other systems, Np showed enhanced sorption compared to the oxic control with >90% Np sorbed after 10 days (Supporting Information Table 1). The XANES spectra for the prereduced sediments exposed to Np(V) showed a clear change from a Np(V)-like spectrum for sterile oxic and denitrifying sediments to a Np(IV)-like spectrum for Fe(III)-, sterile Fe(III)-, progressive Fe(III)-, and sulfate-reducing systems (Figure 2; Supporting Information Table 1) (*38, 44*). This suggests that biotransformation to Np(IV) was complete upon the cessation of Fe(III)-reduction and the absence of Np(IV) in porewaters (<1% total of total $Np_{(aq)}$ in the early metal and Fe(III)-reduced microcosms; (*20*)) indicates that reduction occurred in the sediments. Additionally, the progressively bioreduced system developed Fe(III)-reducing conditions in the presence of 0.2 mM Np, and Np(V) was biotransformed to Np(IV), highlighting the tolerance of the sediment microbial community (Supporting Information Table 6) to low millimolar concentrations of radiotoxic Np. Furthermore, reduction of Np(V) to Np(IV) in the sterile Fe(III)-reducing microcosm highlights that abiotic electron transfer from Fe(II)-bearing sediments to Np(V) occurs and forms poorly soluble Np(IV). This robust bioreduction to Np(IV) is in contrast to some axenic culture studies where Np(V) is not reduced (*9, 11, 13*). This is despite the fact that the Fe(III)-reducing enzymes present in these experiments should be able to reduce Np(V) to Np(IV) (*11*). Interestingly, the early metal-reducing sample showed a XANES spectrum intermediate between Np(V) and Np(IV), suggesting that Np(V) reduction began during manganese and/or early iron reduction (Figure 2). Linear combination modeling of this XANES spectrum was possible with a mixture of Np(IV)- and Np(V)-like end-member spectra, confirming that Np(V) bioreduction was incomplete under these conditions (Supporting Information Table 1). Interpretation of the EXAFS spectra for these samples supported the XANES findings, with a Np(V)-like coordination environment (two oxo oxygen backscatters at ~1.85 Å with four equatorial oxygen backscatters at ~2.5 Å *36−38, 41−43*) evident in the oxic sample and a Np(IV)-like environment (five oxygen backscatters at ~2.34 Å and three oxygen backscatters at ~2.56 Å (*39*)) in the progressively Fe(III)-reduced and sulfate reduced samples (Supporting Information Figure 1 and Supporting Information Table 2). Again, a mixture of both the Np(V) and Np(IV) models provided the best fit for the early metal-reducing sample, confirming that both Np(V) and Np(IV) were present in this sample (see Supporting Information for further modeling information). In all samples, a high amplitude feature was also evident in the Fourier transforms at ~3.50 Å, reflecting a possible Np/Fe contribution in the sediment-associated Np species (*36*) (Supporting Information Figure 1 and Supporting Information Table 2).

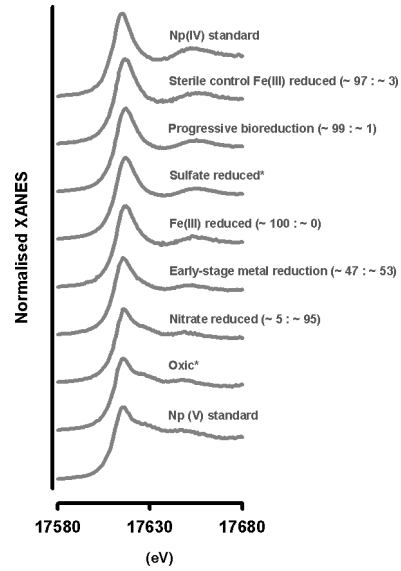

FIGURE 2. Np L_{III}-edge XANES spectra for sediments under different biogeochemical conditions. Representative Np L_{III}-edge XANES spectra for Np(V)- and Np(IV)-aquo standards are shown for comparison. Values in brackets are the estimated Np(IV):Np(V) ratio as determined from linear combination modeling between oxic* (Np(V)-like) and sulfate-reduced* (Np(IV)-like) sediment end-member spectra. Note the structural differences between the Np(V) and Np(IV) standard spectra (and oxic- (Np(V)-like) and sulfate-reduced (Np(IV)-like) sediment spectra). Np(V) XANES spectra have a multiple scattering (MS) resonance structure at the high energy flank of the white line (due to scattering along the axial or 'yl' oxygen atoms of the linear neptunyl moiety); this MS feature is missing in Np(IV) XANES spectra (*38*).

Reoxidation Experiments. At nuclear legacy sites, both air and nitrate (via biologically mediated nitrate reoxidation reactions) may be significant oxidants in the shallow subsurface (*19, 45, 46*). Furthermore, nitrate will be present at high levels in some geological disposal scenarios (*47*). Thus, to further assess the full microbial redox cycle of Np, we performed a constrained set of XAS experiments to define the reoxidation behavior of sediment-associated Np(IV) (Figure 3 and Supporting Information Table 1). Upon air exposure, extractable Fe(II) in the sediment slurry was rapidly oxidized (>90% oxidation after 40 days; Supporting Information Table 1). In contrast, Np(IV) was recalcitrant to remobilization with <20% returned to solution after 40 days as Np(V), and the sediment XANES spectra at this time could be modeled with mixed Np(IV): Np(V) end-member contributions (Figure 3; Supporting Information Table 1). Results from the nitrate reoxidation experiment were broadly similar: >90% of Fe(II) was oxidized after 40 days, and both gas production and transient NO_2^- in porewaters indicated that the reoxidation of Fe(II) was coupled to microbial NO_3^- reduction (Supporting Information Table 1) (*19*). Neptunium remobilization to solution was again very limited (<10%, all as Np(V)), and the sediment XANES spectra could be modeled with mixed Np(IV):Np(V) end-member contributions (Figure 3; Supporting Information Table 1). In contrast, the sterile prereduced control showed no/limited reoxidation of both Fe(II) and Np(IV). Together, these results suggest that Np(IV) reoxidation is incomplete and hindered on exposure to air and nitrate, which contrasts with the extremely fast and

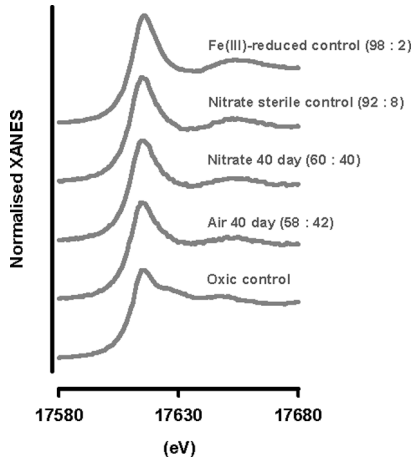

FIGURE 3. Np L_{III}-edge XANES spectra for sediments undergoing air and nitrate reoxidation. Np L_{III}-edge XANES spectra for oxic (Np(V)-like) sediments, and Fe(III)-reduced (Np(IV)-like) sediments are also shown for comparison. Values in brackets are the estimated Np(IV):Np(V) ratio as determined from linear combination modeling between oxic (Np(V)-like) and sulfate reduced (Np(IV)-like) sediment end-member spectra.

almost complete reoxidation of sediment-associated U(IV) under similar conditions (*46*).

Geochemical Significance. Overall, these data provide the first conclusive evidence that nuclear site indigenous microbial communities can mediate the bioreduction of anthropogenic Np(V) to Np(IV), across a range of concentrations. Furthermore, they highlight the complexity of redox cycling processes that can affect Np with both air and nitrate reoxidation experiments suggesting that once Np(IV) is formed, it is surprisingly resistant to reoxidation. These observations have significant implications for contaminated land and geological disposal scenarios in which bioreduction could enhance Np retention. This work highlights the critical importance of understanding biogeochemical processes in the management of the transuranic elements, a significant and highly challenging component of the global nuclear legacy.

Supporting Information Available

Details of synthetic groundwater composition, XAS modeling details, Supporting Information Figure 1: Np L_{III} edge EXAFS and Fourier transforms, Supporting Information Table 1: XAS microcosm geochemical characteristics and XANES linear combination results, Supporting Information Table 2: EXAFS modeling results, and Supporting Information Tables 3−6: 16S rRNA phylogenetic affiliations for bioreduction time-points. This information is available free of charge via the Internet at http://pubs.acs.org/.

Acknowledgments

We thank R. Mortimer, P. Lythgoe, K. Law, B. Brendebach, A. Cowling, and I. Haslam for analytical and safety assistance. This work was supported by NERC grants (NE/D00473X/1, NE/D005361/1) and ANKA/ACTINET and ENVIROSYNC2 awards for work at the INE Beamline, ANKA synchrotron radiation source, Karlsruhe Institute of Technology, Germany.

Literature Cited

(1) Kaszuba, J. P.; Runde, W. H. The aqueous geochemistry of neptunium: dynamic control of soluble concentrations with applications to nuclear waste disposal. *Environ. Sci. Technol.* **1999**, *33*, 4427–4433.

(2) Dozol, M.; Hagemann, R. Radionuclide migration in groundwater: review of the behaviour of actinides. *Pure Appl. Chem.* **1993**, *65*, 1081–1102.

(3) Krauskopf, K. *Radioactive Waste Disposal and Geology.*: Chapman and Hall, New York, 1988.

(4) Lloyd, J. R.; Renshaw, J. C. Microbial transformations of radionuclides: Fundamental mechanisms and biological implications. In: *Metallic Ions in Biological Systems* edited by Sigel, A.; Sigel, H.; Sigel, R. K. O., Eds.; M. Dekker, New York., 2005, *43*, 205−240.

(5) Wu, T.; Amayri, S.; Drebert, J.; van Loon, L. R.; Reich, T. Neptunium (V) sorption and diffusion in opalinus clay. *Environ. Sci. Technol.* **2009**, *43*, 6567–6671.

(6) Ehrlich, H. L. *Geomicrobiology*; CRC Press: Boca Raton, FL, 2009.

(7) Konhauser, K. O. *Introduction to Geomicrobiology*; Blackwell: Oxford, 2007.

(8) Lovley, D. R.; Phillips, E. J. P.; Gorby, Y. A.; Landa, E. R. Microbial reduction of uranium. *Nature* **1991**, *350*, 413–416.

(9) Lloyd, J. R.; Yong, P.; Macaskie, L. E. Biological reduction and removal of pentavalent Np by the concerted action of two microorganisms. *Environ. Sci. Technol.* **2000**, *34*, 1297–1301.

(10) Rittmann, B. E.; Babaszak, J. E.; Reed, D. T. Reduction of Np(V) and precipitation of Np(IV) by an anaerobic microbial consortium. *Biodegradation* **2002**, *13*, 329–342.

(11) Renshaw, J. C.; Butchins, L. J. C.; Livens, F. R.; May, I.; Charnock, J. M.; Lloyd, J. R. Bioreduction of uranium: environmental implications of a pentavalent intermediate. *Environ. Sci. Technol.* **2005**, *39*, 5657–5660.

(12) Boukhalfa, H.; Icopini, G. A.; Reilly, S. D.; Neu, M. P. Plutonium(IV) reduction by the metal-reducing bacteria *Geobacter metallireducens* GS15 and *Shewanella oneidensis* MR1. *Appl. Environ. Microbiol.* **2007**, *73*, 5897–5903.

(13) Icopini, G. A.; Boukhalfa, H.; Neu, M. P. Biological reduction of Np(V) and Np(V) citrate by metal-reducing bacteria. *Environ. Sci. Technol.* **2007**, *41*, 2764–2769.

(14) Reed, D. T.; Pepper, S. E.; Richmann, M. K.; Smith, G.; Deo, R.; Rittmann, B. E. Subsurface bio-mediated reduction of higher-valent uranium and plutonium. *J. Alloy Compound* **2007**, *444/445*, 376–382.

(15) Renshaw, J. C.; Law, N.; Geissler, A.; Livens, F. R.; Lloyd, J. R. Impact of the Fe(III)-reducing bacteria *Geobacter sulfurreducens* and *Shewanella oneidensis* on the speciation of plutonium. *Biogeochemistry* **2009**, *94*, 191–196.

(16) Law, G. T. W.; Geissler, A.; Boothman, C.; Burke, I. T.; Livens, F. R.; Lloyd, J. R.; Morris, K. Role of nitrate in conditioning aquifer sediments for technetium bioreduction. *Environ. Sci. Technol.* **2010**, *44*, 150–155.

(17) Katz, J. J.; Seaborg, G. T.; Morss, L. R. *The Chemistry of the Actinide Elements*, 2nd ed.; Chapman Hall: London, 1986.

(18) Wilkins, M. J.; Livens, F. R.; Vaughan, D. J.; Beadle, I.; Lloyd, J. R. The Influence of Microbial Redox Cycling on Radionuclide Mobility in the Subsurface at a Low-Level Radioactive Waste Storage Site. *Geobiology* **2007**, *5*, 293–301.

(19) Burke, I. T.; Boothman, C.; Lloyd, J. R.; Livens, F. R.; Charnock, J. M.; McBeth, J. M.; Mortimer, R. J. G.; Morris, K. Reoxidation Behavior of Technetium, Iron, and Sulfur in Estuarine Sediments. *Environ. Sci. Technol.* **2006**, *40*, 3529–3535.

(20) Bertrand, A.; Choppin, G. R. Separation of actinides in different oxidation states by solvent extraction. *Radiochim. Acta* **1982**, *31*, 135.

(21) Viollier, E.; Hunter, P. W.; Roychoudhury, K.; Van Cappellen, P. The ferrozine method revisited: Fe(II)/Fe(III) determination in natural waters. *Appl. Geochem.* **2000**, *15*, 785–790.

(22) Brewer, P. G.; Spencer, D. W. Colorimetric determination of manganese in anoxic waters. *Limnol. Oceanogr.* **1971**, *16*, 107–110.

(23) Harris, S. J.; Mortimer, R. J. G. Determination of nitrate in small volume samples (100 μl) by the cadmium-copper reduction method: a manual technique with application to the interstitial waters of marine sediments. *Int. J. Environ. Anal. Chem.* **2002**, *82*, 369–376.

(24) Burke, I. T.; Boothman, C.; Lloyd, J. R.; Mortimer, R. J. G.; Morris, K. Technetium solubility during the onset of progressive anoxia. *Environ. Sci. Technol.* **2005**, *39*, 4109–4116.

(25) Lovley, D. R.; Phillips, E. J. P. Rapid assay for microbially reducible ferric iron in aquatic sediments. *Appl. Environ. Microbiol.* **1987**, *53*, 1536–1540.

(26) Ranjard, L.; Poly, F.; Combrisson, J.; Richaume, A.; Gourbiere, F.; Thioulouise, J.; Nazaret, S. Heterogeneous cell density and genetic structure of bacterial pools associated with various soil microenvironments as determined by enumeration and DNA fingerprinting approach (RISA). *Microb. Ecol.* **2000**, *39*, 263–272.

(27) Edwards, U.; Rogall, T.; Blocher, H.; Emde, M.; Bottger, E. C.; et al. Isolation and direct complete nucleotide determination of entire genes. Characterization of a gene coding for 16S ribosomal RNA. *Nucleic Acids Res.* **1989**, *17*, 7843–7853.
(28) Lane, D. J. *Nucleic acid techniques in bacterial systematics*; John Wiley and Sons: New York, 1991.
(29) Zhang, Z.; Schwartz, S.; Wagner, L.; Miller, W. A Greedy Algorithm for Aligning DNA Sequences. *J. Comp. Biol.* **2000**, *7*, 203–214.
(30) Maidak, B. L.; Cole, J. R.; Lilburn, T. G.; Parker, C. T.; Saxman, P. R.; Farris, R. J.; Garrity, G. M.; Olsen, G. J.; Schmidt, T. M.; Tiedje, J. M. The RDP (Ribosomal Database Project) continues. *Nucleic Acids Res.* **2000**, *28*, 173–174.
(31) Denecke, M. A.; Rothe, J.; Dardenne, K.; Blank, H.; Hormes, J. The INE-beamline for actinide research at ANKA. *Phys. Scr.* **2005**, *115*, 1001.
(32) Ravel, B.; Newville, M. ATHENA, ARTEMIS, HEPHAESTUS: data analysis for X-ray absorption spectroscopy using IFEFFIT. *J. Synchrotron Radiat.* **2005**, *12*, 537–541.
(33) Gurman, S. J.; Binsted, N.; Ross, I. A rapid, exact curved-wave theory for EXAFS calculations. *J. Phys. Solid State Phys.* **1984**, *17*, 143–151.
(34) Gurman, S. J.; Binsted, N.; Ross, I. A rapid, exact, curved-wave theory for EXAFS calculations. II. The multiple-scattering. *J. Phys. Solid State Phys.* **1986**, *19*, 1845–1891.
(35) Binsted, N. Excurv98 Program, CCLRC Daresbury Laboratory, 1998.
(36) Combes, J. M.; Chislholm-Brause, C. J.; Brown, G. E., Jr.; Parks, G. A.; Conradson, S. E.; Eller, G.; Triay, I. R.; Hobart, D. E.; Miejer, A. EXAFS spectroscopic study of neptunium (V) sorption at the α-FeOOH water interface. *Environ. Sci. Technol.* **1992**, *26*, 376–382.
(37) Clark, D. L.; Conradson, S. D.; Ekberg, S. A.; Hess, N. J.; Neu, M. P.; Palmer, P. D.; Runde, W.; Tait, C. D. EXAFS studies of pentavalent neptunium carbonato complexes. Structural elucidation of the principal constituents of neptunium in groundwater environments. *J. Am. Chem. Soc.* **1996**, *118*, 2089–2090.
(38) Denecke, M. A.; Dardenne, K.; Marquardt, C. M. Np(IV)/Np(V) valence determinations from Np. L3 edge XANES/EXAFS. *Talanta* **2005**, *65*, 1008–1014.
(39) Llorens, I.; Den Auwer, C.; Mossy, P.; Ansoborlo, E.; Vidaud, C.; Funke, H. Neptunium uptake by serum transferrin. *FEBS J.* **2005**, *272*, 1739–1744.
(40) Moyes, L. N.; Jones, M. J.; Reed, W. A.; Livens, F. R.; Charnock, J. M.; Mosselmans, J. F. W.; Hennig, C.; Vaughan, D. J.; Pattrick, R. A. D. An X-ray absorption spectroscopy study of neptunium (V) reactions with mackinawite (FeS). *Environ. Sci. Technol.* **2002**, *36*, 179–183.
(41) Schmeide, K.; Reich, T.; Sachs, S.; Brendler, V.; Heise, K. H.; Bernhard, G. Neptunium (IV) complexation by humic substances studied by X-ray absorption fine structure spectroscopy. *Radiochim. Acta* **2005**, *93*, 187–196.
(42) Herberling, F.; Denecke, M. A.; Bushbuck, D. Neptunium (V) coprecipitation with calcite. *Environ. Sci. Technol.* **2007**, *42*, 471–476.
(43) Arai, Y.; Moran, P. B.; Honeyman, B. D.; Davis, J. A. *In Situ* spectroscopic evidence for neptunium (V)-carbonate inner sphere and outer sphere ternary surface complexes on hematite surfaces. *Environ. Sci. Technol.* **2007**, *41*, 3940–3944.
(44) Soderholm, L.; Antonio, M. R.; Williams, C.; Wasserman, S. R. XANES Spectroelectrochemistry: A New Method for Determining Formal Potentials. *Anal. Chem.* **1999**, *71* (20), 4622–4628.
(45) Singleton, M. J.; Woods, K. N.; Conrad, M. E.; De Paolo, D. J.; Dresel, P. E. Tracking sources of unsaturated zone and groundwater nitrate contamination using nitrogen and oxygen stable isotopes at the Hanford site, Washington. *Environ. Sci. Technol.* **2005**, *39*, 3563–3570.
(46) Moon, H. S.; Komlos, J.; Jaffe, P. R. Uranium reoxidation in previously bioreduced sediment by dissolved oxygen and nitrate. *Environ. Sci. Technol.* **2007**, *41*, 4587–4592.
(47) Committee on Radioactive Waste Management, Document 2543, 2009.

ES101911V